Future Batteries 9 (2026) 100163

Contents lists available at ScienceDirect

Future Batteries

journal homepage: www.sciencedirect.com/journal/future-batteries

Toward efficient and durable zinc-air batteries via external field manipulation

Tianyu Wang, Maochun Wu *

Department of Mechanical Engineering, The Hong Kong Polytechnic University, Kowloon 999077, Hong Kong Special Administrative Region of China

ARTICLE INFO

Keywords:
Zinc-air batteries
External field modulation
Mass transport
Oxygen electrocatalysis
Zinc dendrite

ABSTRACT

Zinc-air batteries (ZABs) are highly promising candidates for next-generation energy storage systems owing to their high energy density, intrinsic safety, and use of earth-abundant materials. However, their practical implementation is hindered by sluggish oxygen electrochemistry, complex interfacial reactions, and mass transport limitations, which are difficult to overcome through materials-centric optimization strategies alone. The introduction of external fields has emerged as a transformative approach to modulate reaction pathways and interfacial dynamics, thereby enabling significant battery performance enhancements. In this perspective, we critically examine recent advances in deploying various external fields, including magnetic, acoustic, light, stress, microwave, and multi-field coupling to overcome kinetic and transport limitations. We elucidate the fundamental mechanisms underlying these effects, assess their impact on battery performance, and highlight unresolved scientific and engineering challenges. Finally, we outline future directions for external field regulation as a paradigm-shifting strategy toward efficient and durable ZABs.

Introduction

The global transition from fossil fuels to renewable energy sources has accelerated in recent years, driven by rising energy demand and growing environmental concerns [1,2]. However, the inherent intermittency of renewables such as wind and solar leads to fluctuating electricity output, posing significant challenges to grid stability [3]. To ensure a reliable power supply, it is urgently necessary to develop high-performance energy storage systems (EESs) [4,5]. Among various candidates, zinc-air batteries (ZABs) have attracted considerable attention owing to their high theoretical energy density (1086 Wh kg^{-1}), reliance on earth-abundant materials, and intrinsic operational safety [6,7].

Despite their promising prospects, the practical implementation of ZABs remains hindered by several critical challenges. At the negative electrode, dendrite formation, shape change, and side reactions persist as long-standing issues that hinder their long-term operation. It is widely accepted that non-uniform electron distribution and heterogeneous ion flux are the main culprits of zinc dendrite growth, which exacerbates side reactions, generates electrically isolated "dead zinc", and even causes internal short circuits [8]. At the air electrode, a notable challenge lies in the sluggish kinetics of oxygen reduction reaction (ORR) and oxygen evolution reaction (OER), which result in large activation polarizations during charge and discharge processes, leading to low energy efficiencies [9,10]. Moreover, gas bubbles generated by OER during charging tend to adhere to the electrode surface, blocking active sites and obstructing mass transport pathways [11]. This phenomenon increases overpotentials and results in non-uniform current density distribution. The former accelerates electrode degradation while the latter promotes dendrite growth at the negative electrode, both of which lead to rapid performance decay. To overcome these challenges, extensive research efforts have been devoted over the past decades. For the zinc electrode, strategies primarily focus on structural engineering (e.g., design of 3D porous electrodes) and electrolyte formulation (e.g., use of additives or co-solvents) to regulate uniform zinc deposition [12–14]. On the air cathode side, major efforts are devoted to developing efficient bifunctional catalysts, such as single-atom catalysts [15], transition metal-based materials [16], and carbon-based materials [17,18]. Although these approaches have been demonstrated to be effective in improving battery performance to some extent, there remains significant room for improvement. This is because electrochemical reactions are governed by thermodynamic, kinetic, and mass transport factors, which are difficult to regulate through material design alone.

Applying external fields has emerged as an effective approach to

* Corresponding author.
E-mail address: maochun.wu@polyu.edu.hk (M. Wu).

https://doi.org/10.1016/j.fub.2026.100163
Received 31 December 2025; Received in revised form 14 February 2026; Accepted 23 February 2026
Available online 23 February 2026

modulate electrochemical processes. By transferring external forces or high-intensity energy into batteries in a contactless manner, external fields can regulate mass transport, enhance reaction kinetics, and even alter thermodynamic potentials of ZABs, thereby enhancing the overall energy conversion efficiency and lifespan of ZABs. Early studies introduced magnetic fields to induce magnetohydrodynamic (MHD) convection, thereby promoting uniform zinc deposition [19]. Subsequent investigations demonstrated that magnetic field-driven electrolyte motion can facilitate bubble detachment at the air cathode, enhancing charge-transfer kinetics in ZABs [20]. Acoustic fields have also been shown to enhance ionic transport and suppress dendrite formation through cavitation-induced microstreaming effects [21]. More recently, light-assisted ZABs have attracted increasing attention by leveraging photon excitation to alleviate sluggish reaction kinetics and improve round-trip efficiency [22,23]. Beyond these approaches, stress field, microwave field, and multi-field coupling strategies have further broadened the regulatory dimensions of ZABs by tuning catalytic active sites, enabling spatially homogeneous thermal distributions under microwave irradiation, and harnessing synergistic physical interactions to accelerate overall reaction kinetics [24–27]. In this article, we summarize the latest advances in ZABs assisted by magnetic, acoustic, light, stress, microwave, and multi-field strategies and critically analyze the regulatory mechanisms (Fig. 1). The performance benefits arising from the application of external fields are highlighted. More importantly, we offer a critical assessment of the current research landscape, identifying key challenges that impede the advancement of external field-assisted ZABs, including incomplete mechanistic understanding, the nascent state of multiphysics synergistic modulation, and the lack of mature engineering strategies for practical implementation. This perspective aims to clarify emerging research opportunities and provide guidance for the rational design and future development of external field-assisted ZABs.

Magnetic field-assisted ZABs

Magnetic fields, as a facile and non-contact regulation strategy, have attracted considerable attention in advanced EESs [28,29]. In ZABs, the application of an external magnetic field primarily induces the MHD effect driven by the Lorentz force. A typical configuration for generating this effect is depicted in Fig. 2a, where the field is introduced via an electromagnet positioned adjacent to the electrodes. The field strength can be tuned by adjusting either the input current or the magnet-electrode distance. During operation, migrating ions in the electrolyte intersect magnetic flux lines and experience the Lorentz force perpendicular to their trajectories [30], which perturbs ion migration paths and induces localized convection and hydrodynamic micro-disturbances, collectively referred to as the MHD effect [31]. These localized MHD vortices effectively enhance electrolyte convection and mass transport near the electrode surface, reducing concentration polarization and promoting more uniform electrochemical reactions, thereby enhancing battery cycling stability [32,33]. Liang et al [34]. demonstrated that magnetic-field regulation can modulate ion migration pathways in ZABs. When microscopic protrusions form on the zinc electrode surface, local electric-field distortions cause zincate ions to experience the Lorentz force under the applied magnetic field, as illustrated in Fig. 2b. Consequently, the trajectories of zincate ions shift from linear to spiral, inducing microscale vortex flows. Fig. 2c schematically depicts the zinc electrodeposition process under magnetic-field modulation. The MHD-induced micro-convection enhances localized mass transport at the electrode-electrolyte interface, alleviates concentration polarization, and homogenizes ion distribution near surface protrusions, thereby effectively suppressing dendrite growth. In situ observation by Chen et al. further confirmed the dendrite-suppressing capability of magnetic-field regulation [32]. In the absence of a magnetic field, the zinc foil surface exhibited loose and irregular deposition, whereas applying a continuous magnetic field produced a markedly denser and smoother deposition layer. These findings confirm that magnetic-field regulation is an effective strategy for inhibiting dendrite growth and promoting uniform zinc deposition.

In addition to dendrite suppression, magnetic fields can also be applied to address challenges associated with air electrodes in ZABs. The sluggish OER is accompanied by continuous oxygen evolution, and the adherence of oxygen bubbles on the electrode surface can block active sites and restrict electrolyte access, thereby aggravating mass transport limitation and concentration polarization [35,36]. To address these issues, Wang et al [37]. utilized the MHD effect to regulate oxygen bubble behavior in ZABs. By aligning a permanent magnet parallel to the electrode surface, a magnetic field perpendicular to the ionic current was established. Under this configuration, the Lorentz force drives oxygen bubbles to move directionally, effectively suppressing bubble coalescence and accumulation. Notably, the application of the magnetic field induces distinctive vortex and spiral detachment behaviors of the bubbles, as illustrated in Fig. 2d. These phenomena reflect the MHD effect, which significantly enhances internal electrolyte convection and mass transport within the battery, thereby improving the overall energy conversion efficiency.

Apart from mass transport regulation, external magnetic fields can also trigger spin-polarization effects. This phenomenon arises from the modulation of electron spin alignment, resulting in a transition from low- to high-spin states within the coordination environment [38]. This electronic reconfiguration facilitates the formation of radical intermediates and optimizes the binding strength of surface species, thereby promoting rapid oxygen reaction kinetics. For instance, Wang et al [39]. revealed that applying a magnetic field of 1500 Oe promotes the high-spin state of Fe sites (Fig. 2e), which enhances the adsorption of oxygen intermediates and accelerates electron transfer processes. Consequently, ZABs employing high-spin Fe-based catalysts exhibited remarkably improved reaction kinetics, achieving a high power density of 170 mW cm^{-2} along with superior cycling stability. Similarly, Qian et al [40]. provided further evidence of magnetic field-assisted electrocatalysis, demonstrating exceptional OER performance with an ultralow overpotential of 120 mV under an applied magnetic field (Fig. 2f). More importantly, the resulting ZABs delivered a peak power density of 64.1 mW cm^{-2} under a 1.0 T magnetic field (Fig. 2g), underscoring the promise of magnetic-field modulation in improving catalyst activity and device-level performance.

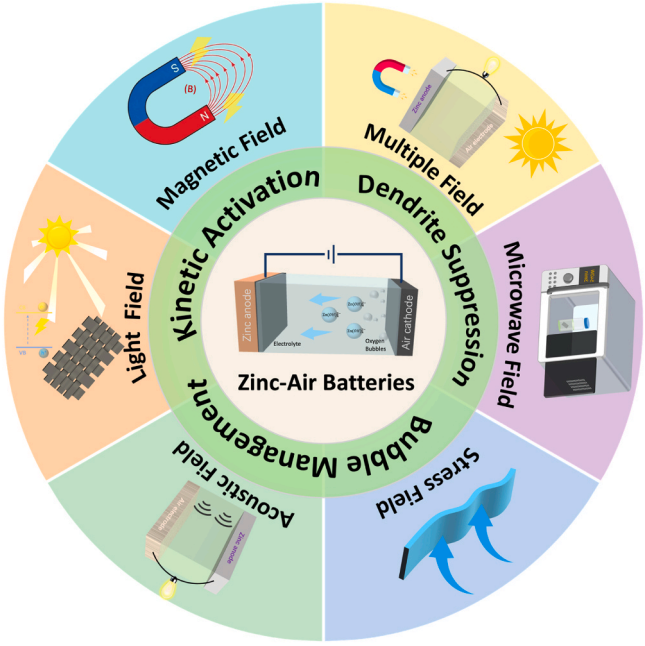

Fig. 1. Overview of ZABs modulated by different external fields.

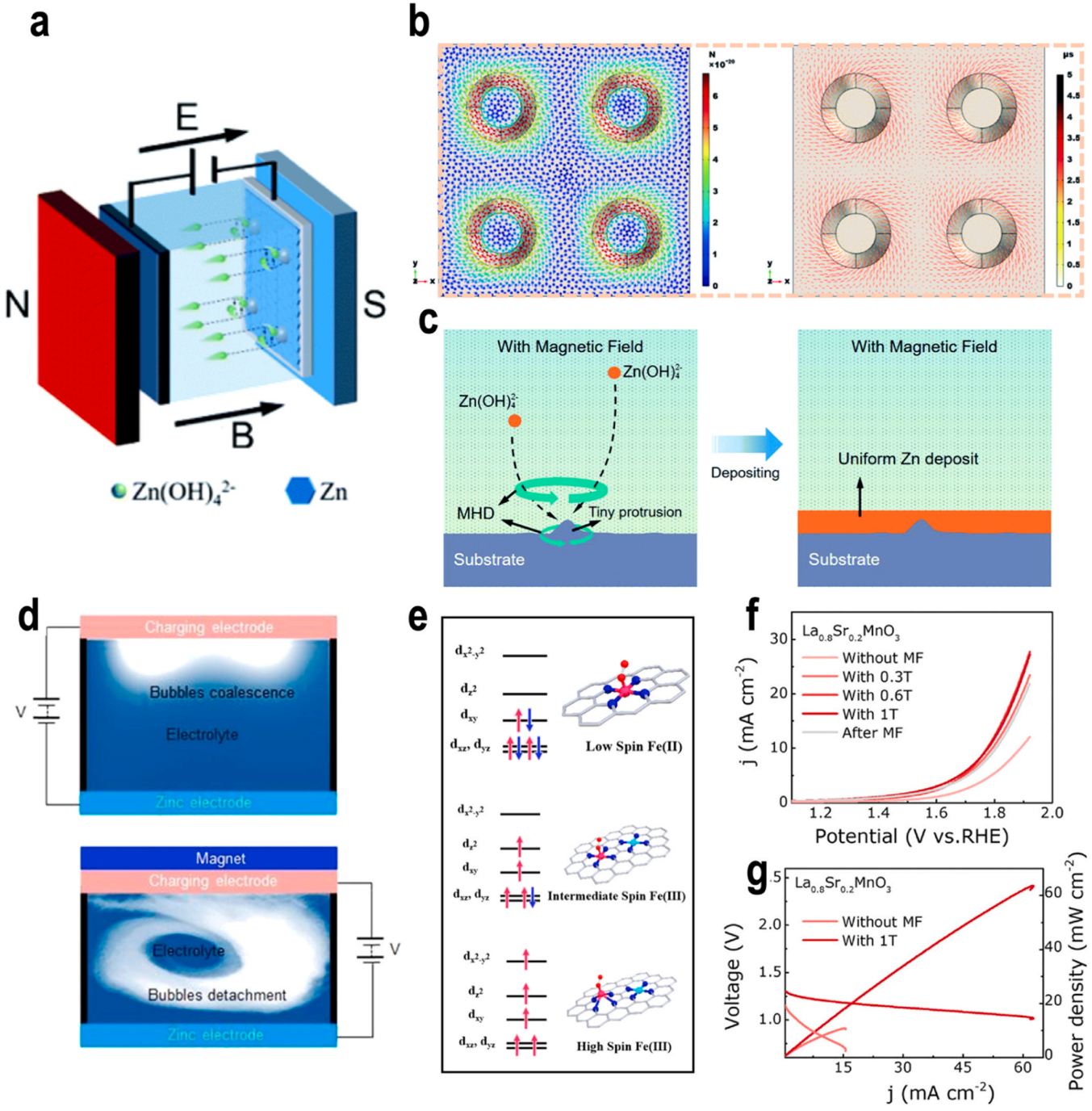

Fig. 2. (a) Schematic diagram of a magnetic-field modulated ZAB. (b) The Lorentz force distribution and trajectories of zincate ions with a magnetic field. (c) Schematic of zinc deposition with a magnetic field. (d) Oxygen detachment with/without a magnetic field. (e) Schematics of spin configuration of the Fe SAs LS, Fe SAs MS and Fe SAs HS. (f) Linear sweep voltammetry (LSV) curves of the catalyst measured at different field strengths. (g) Power density curves of rechargeable ZABs employing the catalyst with/without a magnetic field.
(a) Reproduced from Ref. (b) Reproduced from Ref. (c) Reproduced from Ref. [34] with the permission from Royal Society of Chemistry. (d) Reproduced from Ref. [37] with the permission from Elsevier. (e) Reproduced from Ref. [39] with the permission from Wiley. (f) Reproduced from Ref. (g) Reproduced from Ref. [40] with the permission from Wiley.

Acoustic field-assisted ZABs

Acoustic fields, particularly ultrasonic fields characterized by high frequency and high energy density, offer a promising approach for interfacial modulation in ZABs by enhancing electrolyte flow during charging and discharging processes [41,42]. Electrolyte motion under ultrasonic excitation is primarily driven by three mechanisms, namely acoustic streaming, cavitation-induced turbulence, and microjets. Acoustic streaming, driven by acoustic radiation forces resulting from wave attenuation, generates a steady directional flow that enhances electrolyte replenishment and facilitates byproduct removal. Under intense ultrasonic irradiation, dissolved gases or pre-existing nuclei in the electrolyte can form cavitation bubbles whose rapid expansion and collapse induce turbulence in the bulk electrolyte. When such bubbles collapse asymmetrically near the electrode surface, high-velocity microjets are generated, producing localized interfacial disturbances

and effectively thinning the diffusion layer [43].

Recent studies demonstrate that ultrasonic fields significantly suppress zinc dendrite growth by alleviating zinc-ion concentration polarization near the electrode surface (Fig. 3a). Under ultrasonic excitation, acoustic streaming enhances electrolyte convection and ion replenishment, thereby promoting more homogeneous zinc deposition. Scanning electron microscopy (SEM) images in Fig. 3b reveal compact, uniformly distributed spherical zinc clusters on the electrode surface under acoustic excitation, induced by driving the ultrasonic transducer at an alternating peak-to-peak voltage 35 V (V_{pp}). In contrast, pronounced dendritic and branch-like morphologies are observed in the absence of ultrasonic fields, highlighting the critical role of acoustic regulation in directing zinc deposition behavior [44]. Beyond the anode, ultrasonic fields have also been employed to regulate oxygen bubble behavior at the air cathode. Han et al [45]. systematically investigated oxygen bubble departure under acoustic stimulation (Fig. 3c), revealing that acoustic waves accelerate both bubble nucleation and detachment. This facilitates rapid bubble removal from the electrode surface, effectively mitigating the interfacial resistance caused by the bubble-shielding effect. Experimental results presented in Fig. 3d demonstrate that the OER overpotential is significantly reduced when an ultrasonic field within a frequency of 40 kHz is applied at different temperatures at a current density of 50 mA cm^{-2}. Tafel plots (Fig. 3e) further corroborate these improvements, highlighting the critical role of acoustic fields in optimizing bubble dynamics and boosting reaction kinetics. In addition, ultrasonic fields directly modulate interfacial kinetics by inducing

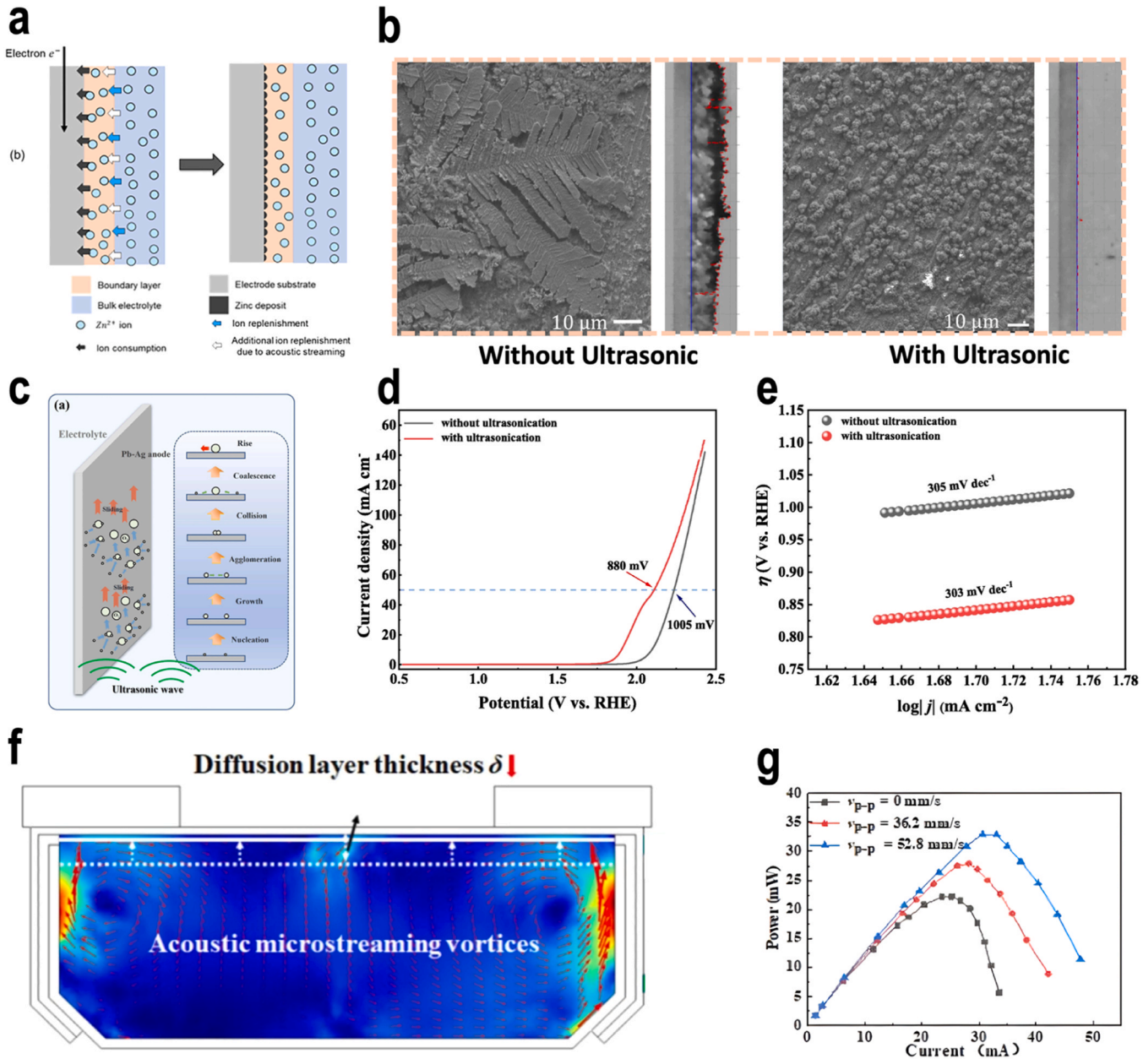

Fig. 3. (a) Mechanism of acoustic streaming that generates additional ion replenishing under an ultrasonic field. (b) Optical images of zinc anodes with/without an ultrasonic field. (c) Schematic depiction of the mechanism for eliminating oxygen bubbles under an ultrasonic field. (d) LSV curves and (e) corresponding Tafel slopes of the electrode with/without an ultrasonic field. (f) Acoustic streaming velocity distribution within the central plane of the internal cavity. (g) Power output curves of the button ZABs.

(a) Reproduced from Ref. (b) Reproduced from Ref. [44] with the permission from Elsevier. (c) Reproduced from Ref. (d) Reproduced from Ref. (e) Reproduced from Ref. [45] with the permission from Elsevier. (f) Reproduced from Ref. (g) Reprduced from Ref. [48] with the permission from MDPI.

acoustic streaming and microturbulence, which perturb the electric double layer (EDL) and facilitate ion exchange, thereby alleviating mass transport limitations and minimizing interfacial resistance [46,47]. For example, Luo et al [48]. pioneered the integration of ultrasonic fields into ZABs by incorporating a piezoelectric ring capable of generating acoustic vibrations. As illustrated in Fig. 3f, the introduction of an internal ultrasonic field generates acoustic streaming vortices, facilitating the removal of ions from the EDL on the electrode surface, thereby mitigating the EDL-induced interfacial transport limitations. Furthermore, variations in acoustic pressure reduce the effective viscosity of the electrolyte, which in turn weakens concentration polarization. As shown in Fig. 3g, at a vibration velocity of 52.8 mm s^{-1} (corresponding to a frequency of 161.2 kHz), the battery achieved a 46.8 % increase in peak output power. Furthermore, ultrasonic excitation further extended discharge duration and enhanced capacity by approximately 20 %, demonstrating its effectiveness in improving ZAB performance under sustained ultrasonic excitation.

Light field-assisted ZABs

Solar energy is widely regarded as one of the most promising alternative energy sources, owing to its sustainability, cost-effectiveness, and broad accessibility [3,49]. By coupling solar energy with ZABs and incorporating photo-responsive catalysts into the air electrode, a light field-assisted ZAB system can be constructed [50]. This emerging strategy not only enables the direct conversion and efficient storage of solar energy but also significantly reduces the charging potential, improves reaction kinetics, and enhances the round-trip efficiency of ZABs under illumination.

The photo-assisted strategy for ZABs, which leverages photogenerated charge carriers, involves integrating semiconductor materials such as TiO_2 [51,52], Fe_2O_3 [53,54] and g-C_3N_4 [55,56] into the air electrode. Upon photoexcitation, these semiconductors generate electron-hole pairs that drive bifunctional photoelectrocatalysis. During discharge, provided that conduction band (CB) of the semiconductor is more negative than the theoretical potential of ORR, photogenerated electrons directly participate in oxygen reduction. This facilitates the conversion of O_2 into intermediates such as O_2^- and OOH^-, and ultimately into the discharge product ZnO, thereby significantly accelerating reaction kinetics and boosting the discharge voltage. For example, Zhu et al [57]. synthesized a polytrithiophene (pTTh) catalyst via electrochemical polymerization. SEM images reveal that pTTh is uniformly coated onto the carbon fiber surface, forming hierarchical spherical structures (Fig. 4a). Based on this air cathode, a photo-responsive ZAB was constructed to achieve the direct conversion of photoenergy into electricity (Fig. 4b). The underlying photo-driven mechanism is elucidated by the energy band diagram in Fig. 4c. Under illumination, pTTh generates photoexcited electrons and holes that efficiently drive the ORR. Consequently, the discharge voltage is elevated to 1.78 V, surpassing the thermodynamic limit of 1.4 V without illumination, thereby significantly boosting the energy output of the battery. During the charging process, the valence band (VB) with a sufficiently positive

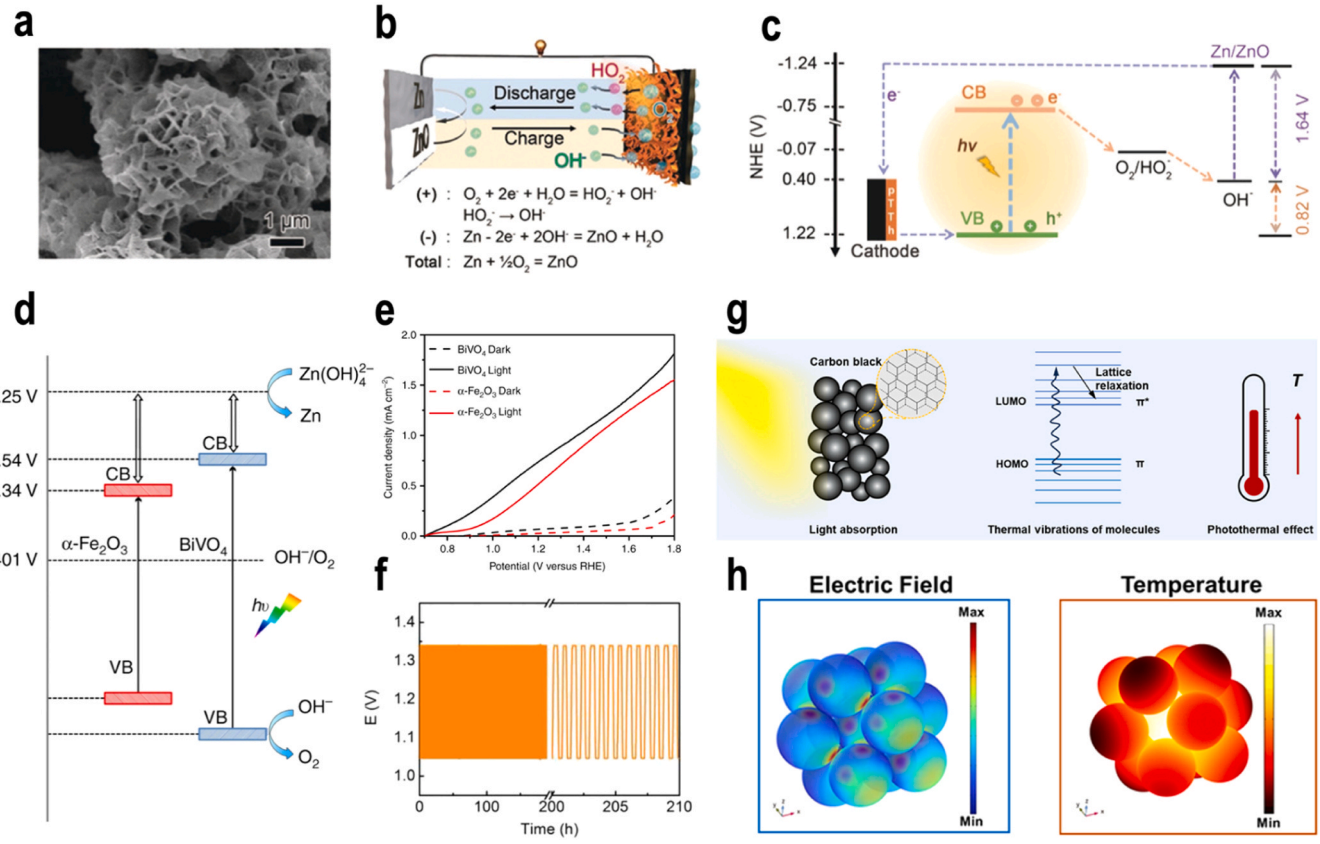

Fig. 4. (a) SEM image of deposited polytrithiophene (pTTh). (b) Schematic of charge and discharge processes of ZABs under illumination. (c) Energy levels responsible for the increased discharge voltage of the ZABs. (d) Mechanism of the sunlight-promoted charging process under illumination. (e) LSV curves of $BiVO_4$ and α-Fe_2O_3 measured with/without illumination. (f) Cycling performance of sunlight-promoted rechargeable ZABs using the TiO_2@In_2Se_3@Ag_3PO_4 air photoelectrode. (g) Mechanism diagram of cathode materials for the photothermal effect under sunlight illumination. (h) 3D electric and temperature field distribution for seven Ni-Mn_3O_4/N-rGo NPs via finite-element method (FEM) modeling.
(a) Reproduced from Ref. (b) Reproduced from Ref. (c) Reproduced from Ref. [57] with the permission from Wiley. (d) Reproduced from Ref. (e) Reproduced from Ref. [23] with the permission from Nature. (f) Reproduced from Ref. [58] with the permission from Elsevier. (g) Reproduced from Ref. [22] with the permission from American Chemical Society. (h) Reproduced from Ref. [60] with the permission from Wiley.

potential ensures that photogenerated holes possess strong oxidative capability, which enables ZnO decomposition and accelerates the conversion of key OER intermediates, thereby lowering the reaction energy barrier and significantly reducing the charging overpotential. Liu et al [23]. further highlighted that the band structure and photoelectrochemical stability of the photoelectrode are critical factors governing the performance of photo-assisted ZABs (Fig. 4d). As shown in Fig. 4e, the α-Fe_2O_3 photocatalyst exhibits excellent performance under 100 mW cm^{-2} illumination, achieving a charging potential as low as approximately 1.43 V. Notably, Feng et al [58]. developed a photo-activated TiO_2@In_2Se_3@Ag_3PO_4 air electrode, enabling ZABs to sustain discharge and charge voltages of 1.34 V and 1.04 V for more than 200 h under 90 mW cm^{-2} light irradiation, highlighting its great potential as a stable and efficient air photoelectrode (Fig. 4f).

Furthermore, illumination induces a pronounced photothermal effect at the electrode, wherein absorbed light is predominantly dissipated through non-radiative relaxation into thermal energy, resulting in a localized temperature increase at the electrode-electrolyte interface. This thermal effect accelerates the reaction kinetics of both the OER and ORR while mitigating polarization losses [59]. As illustrated in Fig. 4g, photoexcitation from highest occupied molecular orbital (HOMO, π) to the lowest unoccupied molecular orbital (LUMO, π^*) state is followed by lattice relaxation, enabling efficient heat generation [22]. The Ni-M-n_3O_4/N-rGo catalyst further exhibits a strong photothermal effect, enabling efficient transformation of absorbed light energy into heat [60]. When employed as the air electrode in ZABs, it significantly narrows the voltage gap to 0.685 V and maintains stable long-term cycling for over 430 cycles even at −10 ℃. Consequently, the synergistic interplay between photothermal effects and photogenerated carrier mechanisms establishes a kinetically favorable environment at the reaction interface, offering a promising pathway to enhance ZAB performance under illumination [61].

Other emerging external fields in ZABs

Beyond the aforementioned magnetic, acoustic, and light modulation strategies, several emerging external fields offer additional opportunities for optimizing ZABs, although research in this domain remains in its infancy. This section highlights recent advances in stress, microwave, and multi-field coupling strategies, which collectively expand the regulatory dimensions of ZABs and provide new avenues for enhancing overall electrochemical performance.

Stress field-assisted ZABs

Stress fields provide a unique strategy for interfacial modulation in ZABs by coupling mechanical deformation with electrochemical processes. At the air cathode, applied stress triggers lattice distortion,

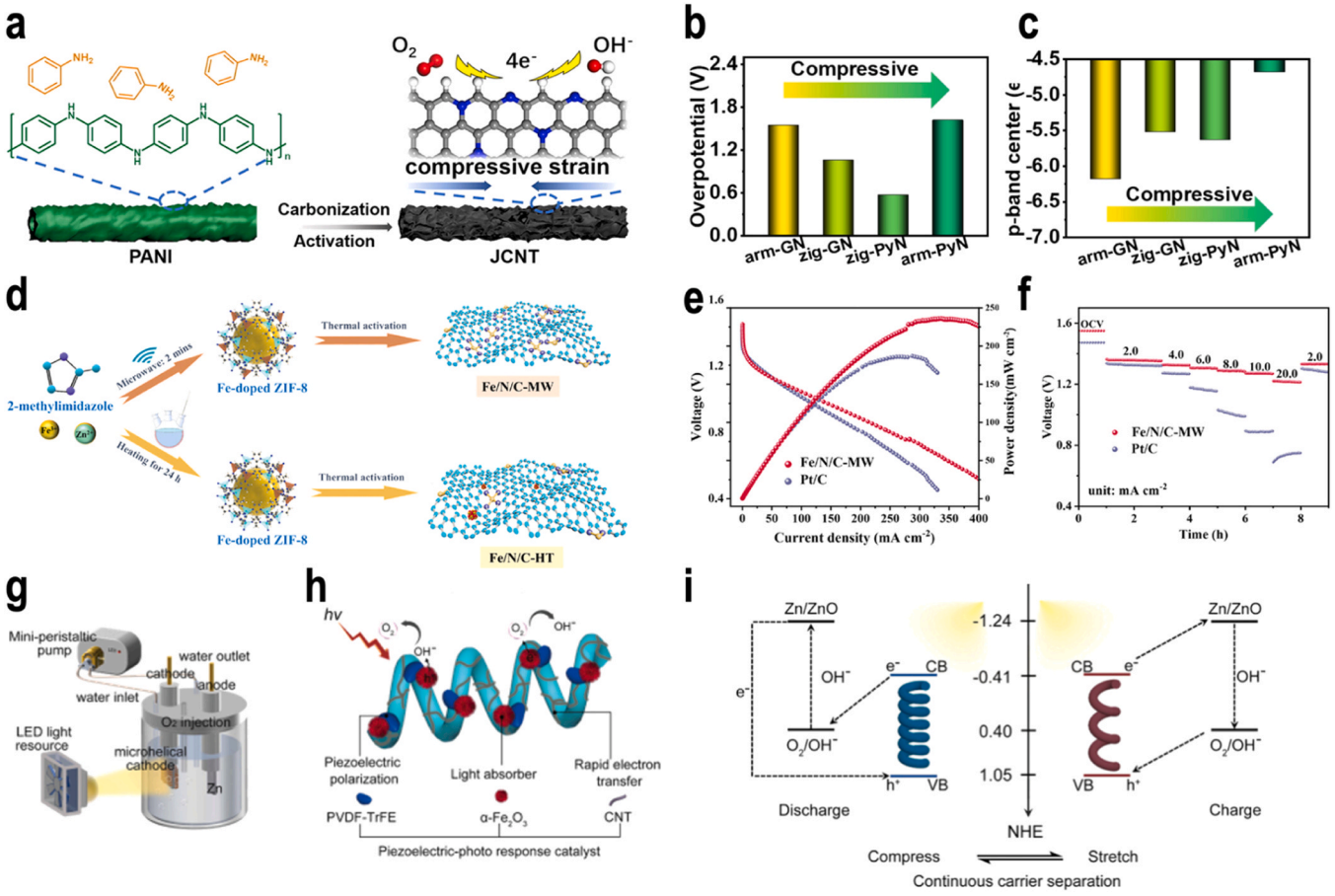

Fig. 5. (a) Schematic illustration of the preparation of JCNTs. (b) Calculated overpotential values for nitrogen-containing zigzag and armchair sites under various strains. (c) p-band centers of armchair and zigzag sites under different compressive strains. (d) Schematic of the synthetic procedures of Fe/N/C-MW and Fe/N/C-HT catalysts. (e) Polarization curves and corresponding power density curves for Fe/N/C-MW ZABs. (f) Discharge profiles of ZABs under different current densities. (g) Diagram of a piezo-photo-assisted ZAB. (h) Schematic of the piezoelectrical-photo response catalyst. (i) Reaction mechanism of the piezoelectric- and photo-assisted ZABs.

(a) Reproduced from Ref. (b) Reproduced from Ref. (c) Reproduced from Ref. [62] with the permission from Elsevier. (d) Reproduced from Ref. (e) Reproduced from Ref. (f) Reproduced from Ref. [64] with the permission from Wiley. (g) Reproduced from Ref. (h) Reproduced from Ref. (i) Reproduced from Ref. [27] with the permission from Wiley.

tuning lattice constants and atomic spacing to govern the rate and selectivity of electrocatalytic reactions. Simultaneously, intrinsic stress optimizes the electronic band structure and electrical conductivity, boosting charge transfer efficiency. Moreover, stress-induced reconstruction of surface atomic configurations and active-site distribution modulates the adsorption energetics of reaction intermediates, thereby facilitating reaction kinetics. Jin et al [62]. fabricated jagged carbon nanotubes (JCNTs) derived from polyaniline grown on carbon nanotubes, as illustrated in Fig. 5a. The intrinsic compressive strain introduced by the jagged architecture effectively lowered the ORR overpotential, with zigzag-pyridinic-N sites exhibiting superior performance (Fig. 5b). Fig. 5c reveals that this enhancement is correlated with the strain-induced modulation of the p-band center, which optimizes the binding energy of oxygen intermediates, ultimately enabling high power density and improved cycling stability in ZABs. Additionally, stress fields demonstrate significant potential for regulating zinc deposition behavior. The introduction of compressive stress effectively elevates the energy barrier for zinc nucleation, suppressing the formation of localized protrusions and thereby retarding dendrite initiation. Simultaneously, a spatially non-uniform stress distribution can induce the preferential zinc deposition along specific directions, enabling crystallographic zinc deposits [63].

Microwave field-assisted ZABs

Microwave fields offer a promising means of energy delivery by leveraging dielectric interactions to provide rapid and volumetric heating in electrochemical systems. This approach greatly reduces energy consumption and shortens synthesis times compared with conventional thermal processes. However, its application in ZABs still remains confined to the synthesis of cathode catalysts at present. For instance, Han et al [64]. employed a microwave-assisted approach to rapidly construct Fe-doped ZIF precursors in only 2 min, producing highly dispersed Fe–N–C single-atom catalysts. As shown in Fig. 5d, this approach significantly promoted the formation and uniform distribution of FeN_4 active sites, enabling ZABs incorporating the optimized catalyst to deliver impressive peak power density and maintain elevated discharge voltages over a wide current-density range, the discharge voltage remaining as high as 1.2 V even at 20 mA cm^{-2}. These findings (Figs. 5e and 5f) highlight the efficacy of microwave-assisted synthesis in enhancing both material structure and electrochemical performance. However, the application of microwave fields during battery operation remains unexplored. Future research could leverage microwave fields for in situ thermal regulation and reaction kinetics control, offering a novel pathway to enhance ZAB performance.

Multi-field assisted ZABs

Although individual external fields have demonstrated notable benefits in regulating electrochemical processes in ZABs, their effects are often confined to single mechanisms and remain insufficient to address the inherently coupled thermodynamic and kinetic constraints of the system. Against this backdrop, multi-field coupling strategies represent a promising research paradigm for ZABs. By integrating two or more external fields, this approach modulates multiscale physical and chemical processes within the battery [65]. Coupling interactions between distinct physical fields enable multidimensional regulation of charge transport, intermediate absorption, and reaction path selectivity, thereby accelerating reaction kinetics, improving mass transport, and enhancing overall battery performance [66].

For instance, the integration of piezoelectric and light fields has emerged as a promising modulation strategy for ZABs. Piezoelectric materials generate a dynamic built-in electric field through piezoelectric polarization under external mechanical deformation, while light fields modulate the electronic structure and spatial distribution of active sites through the photoelectric effect, thereby exciting photogenerated carriers. The coupling of these two fields allows the polarization-induced built-in electric field to regulate photocarrier migration behavior and interfacial energy barriers, achieving synergistic control over charge dynamics and reaction processes. Liang et al [27]. integrated fluid-induced piezoelectric field with light field to develop a piezo-photo-coupled air electrode for ZABs, as illustrated in Fig. 5g. The microhelical cathode, composed of piezoelectric poly (vinylidene fluoride-co-trifluoroethylene) (PVDF-TrFE) and photocatalytic α-Fe_2O_3 (Fig. 5h), undergoes periodic deformation under the impact of flowing fluid, which induces piezoelectric polarization and enables continuous reconstruction of the built-in electric field. This dynamic field continuously drives the spatial separation of photogenerated electron-hole pairs (Fig. 5i), effectively suppressing carrier recombination and accelerating both ORR and OER kinetics. These findings highlight the promise of multi-field coupling strategies for enhancing the electrochemical performance of ZABs. Furthermore, photo-magnetic coupling strategies have been extensively explored for regulating photocarrier dynamics and reaction selectivity under external magnetic fields [67,68]. Under an external magnetic field, electron-hole pairs generated upon light excitation are influenced by the Lorentz force and spin polarization effects, which enhance photocarrier migration and guide oxygen electrochemical reaction pathways through spin-allowed channels. This synergistic regulation suppresses carrier recombination and accelerates oxygen-related reaction kinetics. Although direct experimental validation of photo-magnetic coupling in ZABs remains limited, Xiao et al [69]. demonstrated this strategy in lithium–air batteries, showing that introducing a magnetic field not only enhances the light-absorption capability of semiconductor photocatalysts but also modulates molecular spin states and local electronic structures at the atomic scale, substantially improving photo-responsive behavior. This synergistic interaction fosters superior catalytic activity and accelerates reaction kinetics, offering a rational pathway for designing high-efficiency electrocatalytic systems. Collectively, these emerging physical field strategies underscore the broad potential of multi-field regulation paradigms, offering valuable insights for expanding the regulatory dimensions of ZABs.

Concluding remarks and perspectives

In summary, external field-assisted strategies have progressively advanced from conceptual demonstrations toward in-depth structural design and mechanistic exploration in ZABs, exhibiting unique advantages in achieving multidimensional regulation of reaction thermodynamics and kinetics. This article provides a systematic analysis of the regulatory mechanisms exerted by various external fields, including magnetic, acoustic, light, stress, microwave and multi-field strategies at both the cathode and anode interfaces. Although external-field modulation presents a promising paradigm for overcoming the inherent limitations of conventional material-based strategies and significantly enhancing ZAB performance, its development remains at an early stage, and a comprehensive understanding of system integration and underlying mechanisms is still lacking. The following critical directions are suggested to warrant urgent investigations in the future.

Establishing an in-depth understanding of mechanisms underlying external-field modulation in ZABs

Current research on external field-assisted ZABs remains predominantly focused on analyzing performance enhancements, whereas a systematic and in-depth understanding of the intrinsic mechanisms governing internal reaction processes is still lacking. This gap arises primarily from the inherent complexity of the physicochemical mechanisms induced by external fields. For example, under a magnetic field, the MHD effect not only induces electrolyte convection via the Lorentz force to regulate zincate ion migration but may also alter the spatial distribution of OH^- ions, thereby influencing zinc deposition kinetics and

modifying deposition morphology. The simultaneous action of these intertwined mechanisms leads to nonlinear system responses, highlighting the critical need to disentangle their individual contributions and synergistic interactions under practical operating conditions. Although external field-induced ion redistribution fundamentally reshapes the local interfacial environment, its implications for reaction pathways and intermediate evolution remain insufficiently understood. Addressing these knowledge gaps will require interdisciplinary and systematic investigations. Advanced operando characterization techniques should be employed to track the real-time evolution of electrode interfaces and structural transformations under external fields. Furthermore, numerical simulation methods, such as Molecular Dynamics (MD) and Density Functional Theory (DFT), should be utilized to predict reaction pathway evolution and intermediate species. The combination of experimental and computational insights will enable quantitative validation of mechanistic hypotheses, facilitating the transition of external field-assisted ZAB research from empirical observation to rational, mechanism-driven design.

Investigating material stability and durability in external field–assisted ZABs

Although the introduction of external fields can significantly boost the reaction kinetics of ZABs, systematic investigations into material degradation and failure mechanisms induced by these fields remain insufficient under long-term operation. For instance, prolonged illumination can trigger photo-corrosion, undermining the structural integrity and chemical stability of photo-responsive electrodes. Similarly, the cavitation effect induced by acoustic fields can cause catalyst layer fragmentation, particle detachment, and collapse of porous electrode architectures, accelerating performance deterioration and shortening cycle life. These challenges highlight the necessity for future research on electrode catalyst design that balances high catalytic activity with structural stability and mechanical robustness. Approaches such as band-structure engineering, interfacial reinforcement, and hierarchical architectural design hold promise for achieving more durable catalyst systems. Furthermore, the development of intermittent external-field operation strategies merits in-depth exploration, as such modes may mitigate material stress and parasitic reactions while preserving kinetic benefits.

Rationally integrating multi-field-regulated ZABs

Synergistic regulation through multi-field coupling holds substantial promise for improving the energy efficiency and cycling stability of ZABs. However, current research remains predominantly centered on individual external fields, leaving the exploration of multi-field coupling at an early stage, with many fundamental mechanisms still unresolved. This limitation overlooks the complex synergistic and competitive interactions that can arise among different fields. Future research should therefore aim to elucidate the distinct roles and interaction modes of various external fields in modulating reaction kinetics and interfacial processes. Integrating multiphysics simulations with experimental validation will be essential for unraveling these interactions and enabling the rational design of multi-field-assisted battery systems.

Evaluating practical implementation of external field-enhanced ZABs

Current investigations into external field-assisted ZABs remain predominantly at the laboratory scale, and studies exploring scale-up and practical deployment are still scarce. This gap poses several challenges for practical implementation, including spatial inhomogeneity of field distribution, increased system complexity, and high operational costs. In response to these challenges, future research should prioritize the rational engineering of external field-assisted ZABs, such as optimized magnetic circuits, optical coupling paths, and other field-delivery frameworks to ensure uniform and efficient spatial distribution of external fields within batteries. Advancements in catalyst material synthesis and scalable manufacturing processes are also essential for reducing the cost of electrodes and functional components. These advancements are crucial for transitioning external field-assisted ZABs from laboratory research to real-world commercialization.

CRediT authorship contribution statement

Maochun Wu: Writing – review & editing, Supervision, Funding acquisition, Conceptualization. **Tianyu Wang:** Writing – original draft, Investigation, Conceptualization.

Declaration of Competing Interest

The authors declare that they have no known competing financial interests or personal relationships that could have appeared to influence the work reported in this paper.

Acknowledgements

The work described in this paper was fully supported by the grant from the Research Grants Council of the Hong Kong Special Administrative Region, China (Project No. 16205822).

Data availability

No data was used for the research described in the article.

References

[1] A.M. Omer, Renew. Sust. Energy Rev. 12 (2008) 2265–2300.
[2] H. Chang, X. Liu, A. Xia, W. Zhu, J. Ji, X. Zhu X, J. Zhang, Y. Huang, X. Zhu, Q. Liao, Chem. Soc. Rev. 52 (2026) 1306–1332.
[3] S. Kuşkaya, F. Bilgili, E. Muğaloğlu, K. Khan, M.E. Hoque, N. Toguç, Renew. Energy 206 (2023) 858–871.
[4] C. Ponce de León, A. Frías-Ferrer, J. González-García, D.A. Szánto, J. Power Sources 160 (2006) 716–732.
[5] J. Sun, Z. Guo, L. Pan, X. Fan, L. Wei, T. Zhao, Carb. Neutrality 2 (2023) 30.
[6] Q. Wang, S. Kaushik, X. Xiao, Q. Xu, Chem. Soc. Rev. 52 (2023) 6139–6190.
[7] J. Fu, Z.P. Cano, M.G. Park, A. Yu, M. Fowler, Z. Chen, Adv. Mater. 29 (2017) 1604685.
[8] A. Li, X. Zhang, Z. Xu, M. Wu, Chem. Eng. J. 494 (2024) 153240.
[9] X. Zhong, Y. Shao, B. Chen, C. Li, J. Sheng, X. Xiao, B. Xu, J. Li, H. Cheng, G. Zhou, Adv. Mater. 35 (2023) 2301952.
[10] J. Huang J, Z. Zhao, J. Yu, Y. He, P. Tan, Chem. Asian J. 20 (2025) e202401792.
[11] S. Kroy, W.G. Shin, J. Power Sources 613 (2024) 234820.
[12] Y. Liu, S. Zheng, J. Ma, X. Wang, L. Zhang, P. Das, K. Wang, Z. Wu, Adv. Energy Mater. 12 (2022) 2200341.
[13] A. Li, Z. Xu, X. Zhang, M. Wu, J. Energy Chem. 106 (2025) 688–698.
[14] A. Li, Z. Xu, S.W. Lo, X. Zhang, H. Jiang, M. Wu, Adv. Func. Mater. (2025) e18964.
[15] Y. Wu, Y. Zhao, P. Zhai, C. Wang, J. Gao, L. Sun L, J. Hou, Adv. Mater. 34 (2022) 2202523.
[16] Y. Zhong, Y. Zhang, J. Wang, H. Jin, S. Pan, S. Wang S, Y. Chen, Energy Environ. Sci. 18 (2025) 991–1001.
[17] J. Xue, S. Deng, R. Wang, Y. Li, Carbon 205 (2023) 422–434.
[18] Z. Zhu, P. Liu, P. Du, B. Yu, X. Li, Y. Wang, Ind. Eng. Chem. Res. 62 (2023) 169–179.
[19] A. Bund, S. Koehler, H.H. Kuehnlein, W. Plieth, Electrochim. Acta 49 (2003) 147–152.
[20] J. Shi, H. Xu, L. Lu, X. Sun, Electrochem. Acta 90 (2013) 44–52.
[21] S.J. Banik, R. Akolkar, J. Electrochem. Soc. 160 (2013) D519.
[22] C. Zhao, R. Guo, Y. Zhai, X. Ai, X. Liu, Y. Sun, W. Wang, X. Jin, Q. Zhao, Y. Yang, K. Zhou, M. Wu, ACS Appl. Mater. Interfaces 16 (2024) 63580–63588.
[23] X. Liu, Y. Yuan, J. Liu, B. Liu, X. Chen, J. Ding, X. Han, Y. Deng, C. Zhong, W. Hu, Nat. Commun. 10 (2019) 4767.
[24] J. Wang, X. Zhou, J. Zhao, Y. Cui, F. Yang, P. He, X. Zheng, Mol. Catal. 588 (2026) 115549.
[25] Y. Cha, H. Jang, D. Noh, Y. Seong, J. Choi, T. Kim, J. Seo, J. Kim, J.H. Shim, Y. T. Kang, W. Choi, Adv. Compos. Hybrid. Mater. 8 (2025) 335.
[26] J. Tan, T. Thomas, J. Liu, L. Yang, L. Pan, R. Cao, H. Shen, J. Wang, J. Liu, M. Yang, Chem. Eng. J. 395 (2020) 125151.
[27] S. Liang, L. Song, X. Wang, Y. Wang, J. Wu, H. Wang, J. Xu, Adv. Mater. 36 (2024) 2407718.
[28] L. Zhang, D. Wu, X. Yan, Appl. Phys. Rev. 9 (2022) 031307.
[29] K. Shen, Z. Wang, X. Bi, Y. Ying, D. Zhang, C. Jin C, G. Hou, H. Cao, L. Wu, G. Zheng, Y. Tang, X. Tao, J. Lu, Adv. Energy Mater. 9 (2019) 1900260.

[30] L.M.A. Monzon, J.M.D. Coey, Electrochem. Commun. 42 (2014) 38–41.
[31] M. Bae, M. Kang, Y. Piao, Adv. Funct. Mater. 35 (2025) 2421952.
[32] Q. Chen, C. Jiang, M. Chen, J. Zhang, G. Hou, Y. Tang, Surf. Interfaces 31 (2022) 101972.
[33] D. Yang, J. Qi, G. Sun, T. Wu, R. Gao, Z. Gao, H. Xu, W. Lu, M. Feng, J. Colloid Inter. Sci. 700 (2025) 138454.
[34] P. Liang, Q. Li, L. Chen, Z. Tang, Z. Li, Y. Wang, Y. Tang, C. Han, Z. Lan, C. Zhi, H. Li, J. Mater. Chem. A. 10 (2022) 11971–11979.
[35] C. Zhou, X. Chen, S. Liu, Y. Han, H. Meng, Q. Jiang, S. Zhao, F. Wei, J. Sun, T. Tan, R. Zhang, J. Am. Chem. Soc. 144 (2022) 2694–2704.
[36] A. Bornet, P. Moreno-García, A. Dutta, Y. Kong, M. Liechti, S. Vesztergom, M. Arenz, P. Broekmann, ACS Catal. 14 (2024) 17331–17346.
[37] K. Wang, X. Liu, P. Pei, Y. Xiao, Y. Wang, Chem. Eng. J. 352 (2018) 182–187.
[38] A. Bousseksou, G. Molnár, G. Matouzenko, Eur. J. Inorg. Chem. 2004 (2004) 4353–4369.
[39] Y. Wang, P. Meng, Z. Yang, M. Jiang, J. Yang, H. Li, J. Zhang, B. Sun, C. Fu, Angew. Chem. Int. Ed. 62 (2023) e202304229.
[40] J. Qian, H. Zhang, G. Li, L. Jia, X. Peng, C. Zhong, F. Li, Adv. Funct. Mater. 34 (2024) 2305621.
[41] J. Zhang, Z. Zhou, Y. Wang, Q. Chen, G. Hou, Y. Tang, Nano Energy 102 (2022) 107655.
[42] H. Huang, P. Liu, Q. Ma, Z. Tang, M. Wang, J. Hu, Ultrason. Sonochem. 88 (2022) 106104.
[43] J. Klima, Ultrasonics 51 (2011) 202–209.
[44] Y. Zhang, H. Dong, R. Yang, H. He, G. He, F. Cegla, Electrochem. Commun. 162 (2024) 107700.
[45] G. Han, Z. Chen, N. Cui, S. Yang, Y. Huang, B. Liu, H. Sun, Ultrason. Sonochem. 112 (2025) 107183.
[46] S. Li, C. Wang, C. Chen, Electrochim. Acta 54 (2009) 3877–3883.
[47] F. Foroughi, C.I. Bernäcker, L. Röntzsch, B.G. Pollet, Ultrason. Sonochem. 84 (2022) 105979.
[48] Z. Luo, Q. Tang, J. Hu, Micromachines 12 (2021) 792.
[49] X. Yuan, Y. Wei, H. Yang, Appl. Energy 401 (2025) 126600.
[50] X. Sun, S. Jiang, H. Huang, H. Li, B. Jia, T. Ma, Angew. Chem. 134 (2022) e202204880.
[51] M. Guo, Z. Huang, Y. Qu, L. Wang, H. Li, T.T. Isimjan, X. Yang, Appl. Catal. B Environ. 320 (2023) 121991.
[52] L. Long, Y. Ding, N. Liang, J. Liu, F. Liu, S. Huang, Y. Meng, Small 19 (2023) 2300519.
[53] Q. Dong, S. Ji, H. Wang, V. Linkov, R. Wang, ACS Appl. Mater. Interfaces 14 (2022) 51222–51233.
[54] X. Guo, S. Liu, X. Wan, J. Zhang, Y. Liu, X. Zheng, Q. Kong, Z. Jin, Nano Lett. 22 (2022) 4879–4887.
[55] H. Hayat, T. Noor, N. Iqbal, R. Ahmed, N. Zaman, Y. Huang, J. Environ. Chem. Eng. 11 (2023) 109627.
[56] R. Ren, G. Liu, J.Y. Kim, R.E.A. Ardhi, M.X. Tran, W. Yang, J.K. Lee, Appl. Catal. B Environ. 306 (2022) 121096.
[57] D. Zhu, Q. Zhao, G. Fan, S. Zhao, L. Wang, F. Li, J. Chen, Angew. Chem. Int. Ed. 58 (2019) 12460–12464.
[58] H. Feng, C. Zhang, Z. Liu, J. Sang, S. Xue, P.K. Chu, Chem. Eng. J. 434 (2022) 134650.
[59] R. Cao, L. Liu, W. Yu, S. Ding, SusMat 5 (2025) e251.
[60] W. Guo, F. Gu, Q. Chen, K. Fu, Y. Zhong, J. Lv, S. Pan, Y. Chen, Carbon Energy 6 (2024) e567.
[61] Z. Yuan, H. Mao, D. Yu, X. Chen, Chem. Eur. J. 29 (2023) e202202920.
[62] C. Jin, H. Deng, J. Zhang, Y. Hao, J. Liu, Chem. Eng. J. 434 (2022) 134617.
[63] Y. Li, C.B. Musgrave III, M.Y. Yang, M.M. Kim, K. Zhang, M. Tamtaji, Y. Cai, T. W. Tang, J. Wang, B. Yuan, W.A. Goddard III, Z. Luo, Adv. Energy Mater. 14 (2024) 2303047.
[64] Y. Han, Q. Wei, Y. Fu, D. Zhang, P. Li, X. Shan, H. Yang, X. Zhan, X. Liu, W. Yang, Small 19 (2023) 2300683.
[65] W. Wang, Y. Lu, SusMat 3 (2023) 146–159.
[66] Z. Wang, Y. Li, C. Wu, S.C.E. Tsang, Joule 6 (2022) 1798–1825.
[67] S. Liang, L. Zheng, L. Song, X. Wang, W. Tu, J. Xu, Adv. Mater. 36 (2024) 2307790.
[68] X. Yuan, D. Guan, X. Wang, J. Li, C. Miao, J. Xu, Angew. Chem. 137 (2025) e202421361.
[69] N. Xiao, P. Han, Z. Chen, Q. Chen, J. Colloid Interface Sci. 680 (2025) 911–927.